THE JOURNAL OF BIOLOGICAL CHEMISTRY VOL. 284, NO. 52, pp. 36511–36520, December 25, 2009

RNA Interference in *Trypanosoma brucei*

*ROLE OF THE N-TERMINAL RGG DOMAIN AND THE POLYRIBOSOME ASSOCIATION OF ARGONAUTE**[S]

Received for publication, October 5, 2009, and in revised form, October 29, 2009 Published, JBC Papers in Press, October 30, 2009, DOI 10.1074/jbc.M109.073072

Huafang Shi[‡1], **Nathalie Chamond**[‡1,2], **Appolinaire Djikeng**[‡3], **Christian Tschudi**[§4], **and Elisabetta Ullu**[‡¶]

From the Departments of [‡]*Internal Medicine,* [§]*Epidemiology and Public Health, and* [¶]*Cell Biology, Yale University Medical School, New Haven, Connecticut 06536-8012*

Argonaute proteins (AGOs) are central to RNA interference (RNAi) and related silencing pathways. At the core of the RNAi pathway in the ancient parasitic eukaryote *Trypanosoma brucei* is a single Argonaute protein, *Tb*AGO1, with an established role in the destruction of potentially harmful retroposon transcripts. One notable feature of *Tb*AGO1 is that a fraction sediments with polyribosomes, and this association is facilitated by an arginine/glycine-rich domain (RGG domain) at the N terminus of the protein. Here we report that reducing the size of the RGG domain and, in particular, mutating all arginine residues severely reduced the association of *Tb*AGO1 with polyribosomes and RNAi-induced cleavage of mRNA. However, these mutations did not change the cellular localization of Argonaute and did not affect the accumulation of single-stranded siRNAs, an essential step in the activation of the RNA-induced silencing complex. We further show that mRNA on polyribosomes can be targeted for degradation, although this alliance is not a pre-requisite. Finally, sequestering tubulin mRNAs from translation with antisense morpholino oligonucleotides reduced the RNAi response indicating that mRNAs not engaged in translation may be less accessible to the RNAi machinery. We conclude that the association of the RNAi machinery and target mRNA on polyribosomes promotes an efficient RNAi response. This mechanism may represent an ancient adaptation to ensure that retroposon transcripts are efficiently destroyed, if they become associated with the translational apparatus.

In recent years small 20- to 30-nucleotide-long regulatory RNAs, including small interfering RNAs (siRNAs),[5] micro RNAs (miRNAs), and PIWI-associated RNAs, have emerged as key mediators of a variety of gene-silencing mechanisms operating both at transcriptional and post-transcriptional levels (1). These small RNAs, in a complex with a member of the Argonaute (AGO) or Piwi protein family, act as guides to identify target transcripts. Members of the AGO protein family are present throughout the eukaryotic lineage, from protozoa to man (2), and the family is defined by four distinct domains: the N-terminal, PAZ, MID, and PIWI domains (3, 4). The MID and PAZ domains form binding pockets for the 5′-phosphate and the 3′-end of the guide small RNA, respectively, whereas the PIWI domain adopts a fold similar to that of RNase H-type enzymes. However, only a subset of AGO family members, termed "slicers," are endowed with endonuclease activity. The founding member of the AGO-slicer family is mammalian AGO2 (5, 6), the catalytic engine of the RNA-induced silencing complex or RISC (7). In the classic RNA interference (RNAi) pathway AGO slicers are loaded with siRNAs that guide degradation of target transcripts. Lastly, the MID domain of certain metazoan AGO proteins contains a conserved motif similar to the m^7G cap-binding motif of eukaryotic translation initiation factor 4E, and it has been proposed that human AGO2 may repress translation initiation by sequestering the m^7G-cap of mRNA (8). However, the molecular details of the underlying mechanism remain controversial (9, 10).

At present the function of the N-terminal domain of Argonaute proteins is not well understood, although there is some evidence that this domain plays an important role. For instance, genetic analyses of patterning and morphogenesis in *Drosophila* embryos have revealed an essential role for the N-terminal glutamine-rich repeats of AGO2-slicer (11) and the N-terminal half of *Schizosaccharomyces pombe* AGO1, including the PAZ domain, has been shown to bind to proteins involved in cell-cycle regulation (12). Furthermore, *in vivo* studies from our laboratory have indicated that the N-terminal 68 amino acids of *Trypanosoma brucei* AGO1 (termed the RGG domain, because it includes ten arginine-glycine-glycine or RGG motifs) is an important determinant for the RNAi response (13). More recently, murine Piwi family proteins were found to have methylated arginines in their N termini (14, 15), and these modifications guide interactions with Tudor proteins (15). Finally, the *Drosophila* protein methyltransferase 5 is required for arginine methylation of AGO3 and Aubergine (14).

The RNAi pathway in *Trypanosoma brucei* is controlled by a single Argonaute protein, *Tb*AGO1, which presides over the destruction of potentially dangerous transcripts derived from

* This work was supported, in whole or in part, by National Institutes of Health Grants AI28798 (to E. U.) and AI43594 (to C. T.).

[S] The on-line version of this article (available at http://www.jbc.org) contains supplemental Figs. 1–3.

[1] Both authors contributed equally to this work.

[2] Current address: Laboratoire de Cristallographie et RMN Biologiques UMR8015, Université Paris Descartes, 4 avenue de l'Observatoire, 75270 Paris cedex 06, France.

[3] Current address: The J. Craig Venter Institute, 9704 Medical Center Dr., Rockville, MD 20850.

[4] To whom correspondence should be addressed: 295 Congress Ave., BCMM 136C, Box 9812, New Haven, CT 06536-8012. Tel.: 203-785-7332; Fax: 203-785-7329; E-mail: christian.tschudi@yale.edu.

[5] The abbreviations used are: siRNA, small interfering RNA; miRNA, micro RNA; PRMT, protein arginine methyltransferase; RGG, arginine-glycine-glycine; RISC, RNA-induced silencing complex; RNAi, RNA interference; dsRNA, double-stranded RNA; AGO, Argonaute protein; *Tb*AGO1, *T. brucei* AGO1; UTR, untranslated region; MALDI-TOF, matrix-assisted laser desorption ionization time-of-flight.

retroposons (16). *Tb*AGO1 functions as a "slicer" and conforms to the consensus AGO domain structure (13, 17), except that the MID domain appears to lack the putative m^7G-cap binding motif.[6] Previously, we reported that a proportion of *Tb*AGO1, in a complex with siRNAs, is associated with polyribosomes (13, 18) and that this association is sensitive to inhibition by pactamycin, an inhibitor of early steps in translation initiation. Furthermore, a fraction of siRNAs co-sedimented with translating 80 S ribosomes after limited micrococcal nuclease digestion and deletion of the *Tb*AGO1 RGG domain significantly decreased the association of *Tb*AGO1 with polyribosomes (13). Thus, our previous studies suggested a potential interaction between *Tb*AGO1 and ribosomes.

Although studies *in vitro* and *in vivo* have shown that RNAi can be uncoupled from translation (19–21), a link between the RNAi machinery and the translational apparatus has been suggested by several lines of investigations. Early studies indicated that in S2 cells RISC components pellet with ribosomes and other large complexes after high speed centrifugation (5, 22, 23) and later experiments suggested that RISC is loaded into an 80 S complex, possibly the ribosome (24). Furthermore, two *Drosophila* RISC components, AGO2 and dFXR, were found in complexes containing 5 S rRNA, as well as two ribosomal proteins, L5 and L11 (25). Lastly, in *Drosophila* oocytes, untranslated mRNAs were resistant to RNAi, whereas translated mRNAs were not (26), suggesting that translated mRNAs may be more efficiently targeted by the RNAi machinery. On the other hand, a clear connection between the miRNA pathway and translation has been forged in the last few years (27). In animals, miRNAs in a complex with an AGO-family member (miRISC) mostly mediate translational repression of target mRNAs to which they bind, but translational activation has also been reported (28). Although the mechanism of miRISC-mediated translational repression is still debated, recent studies clearly show that miRNAs are associated with translated mRNA in HeLa cells and are found in polyribosomes (29, 30). Intriguingly, as human AGO2-slicer forms complexes with siRNAs or miRNAs (6), it appears that siRNA- and miRNA-mediated pathways can overlap. Whether siRISC, like miRISC, can recognize and slice target mRNA, while being translated has not been addressed.

Here we report on the functional analysis of the *Tb*AGO1 N-terminal RGG domain and provide further evidence that the association of *Tb*AGO1 with polyribosomes is of functional significance for RNAi-mediated degradation of mRNA. Moreover, we show that mRNA cleavage can occur on polyribosomes stabilized by cycloheximide, although mRNA association with ribosomes is not a pre-requisite for slicing to occur.

EXPERIMENTAL PROCEDURES

Trypanosome Cell Lines—Procyclic cells of strain *T. brucei rhodesiense* YTat1.1 were maintained at 27 °C and transfected as previously described (16).

Construction of AGO1 Mutants—Deletion constructs were generated either by PCR or by overlapping oligonucleotides and cloned into an AGO1 complementation vector (13). Similarly, substitutions of all the arginine residues in the RGG domain were constructed by overlapping oligonucleotides. All mutant constructs were verified by DNA sequencing.

Polyribosome Analysis—Cytoplasmic extracts were prepared by detergent lysis and manual homogenization in polysome buffer (120 mM KCl, 20 mM Tris, pH 7.5, 2 mM $MgCl_2$, 1 mM dithiothreitol, and 10 μg/ml leupeptin) containing 1.2% Nonidet P-40. The lysate was cleared by centrifugation for 4 min at 14,000 rpm and the post-nuclear supernatant was further fractionated into soluble and high speed pellet fractions by centrifugation at 200,000 $\times$ *g* for 1 h. Cycloheximide or pactamycin were added to cells prior to collecting the cells by centrifugation and were present in all buffers throughout the entire procedure. S-200 supernatants were layered onto 15–50% sucrose gradients in polysome buffer and centrifuged for 2 h at 36,000 rpm in a Beckman SW-41 rotor at 4 °C. 1-ml fractions were collected using the ISCO gradient fractionation system. The A_{254} profile was recorded using the ISCO UA-6 detector. Each fraction was precipitated with 1 ml of isopropanol, and the material was collected by centrifugation. Pellets were resuspended in 0.3 ml of a solution containing 10 mM Tris-HCl (pH 7.5), 1 mM EDTA, 100 μg/ml proteinase K, and 1% SDS and incubated at 65 °C for 30 min. Solubilized and digested materials were centrifuged through a microcon-100 filtration unit according to the manufacturer's instructions (Millipore Corp.), and the filtrate was precipitated with 1 volume of isopropanol after addition of 20 μg of glycogen and NaCl to 600 mM. Samples were then processed for Northern blot analysis as described previously (31).

Mass Spectrometry Analysis—TAP-tagged AGO1 from the procyclic form of *T. brucei* was purified as described (32). The TAP-AGO1 fractions were pooled and further fractionated by SDS-PAGE on a 6% polyacrylamide gel. The band corresponding to TAP-tagged AGO1 was excised from the gel and subjected to matrix-assisted laser desorption ionization time-of-flight (MALDI-TOF) mass spectrometry at the W. M. Keck Facility at Yale University.

Subcellular Fractionation—The Qproteome™ Cell Compartment Kit from Qiagen was used for cell fractionation experiments following the protocol provided by the supplier. Equivalent fractions were loaded on 6% SDS-polyacrylamide gels, and the gels were blotted onto Hybond-P (Amersham Biosciences) and probed with rabbit polyclonal antibodies against *Tb*AGO1 (16), Hsp83 (Hsp90 homologue, gift from Jay Bangs, University of Wisconsin), BiP (gift from Jay Bangs, University of Wisconsin (33)), or TbISWI-C (gift from Gloria Rudenko, University of Oxford, UK (34)).

Other Procedures—RNA extraction, dsRNA transfection, and Northern blot analysis were performed as described previously (31). Wild-type and mutant cell lines were challenged with 0, 1, 2, and 10 μg of double-stranded RNA targeting the 5′ UTR of α-tubulin mRNA. To probe the structure of siRNAs, an S-100 extract was treated with proteinase K at room temperature and phenol-extracted, and total RNA, with or without incubation at 95 °C for 2 min, was separated by electrophoresis through 15% polyacrylamide gels. Immunoprecipitations and Western blot analysis were performed as described previously

[6] H. Shi, N. Chamond, A. Djikeng, C. Tschudi, and E. Ullu, unpublished observation.

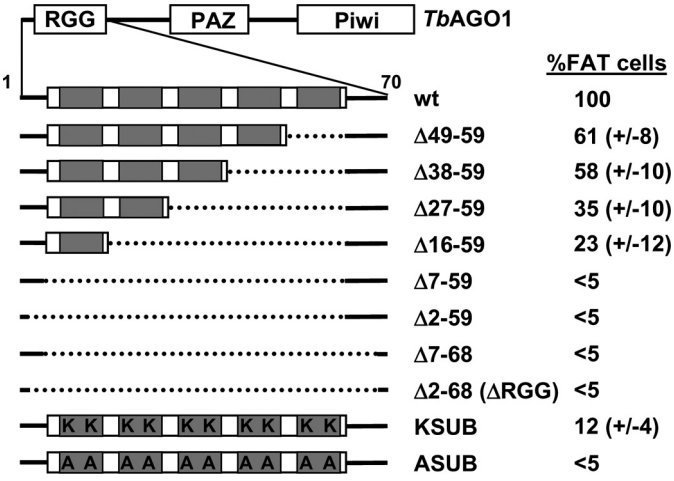

FIGURE 1. **Mutations in the RGG domain affect the RNAi response.** Schematic diagram of *T. brucei* AGO1 and mutant derivatives. The first 70 amino acids, including the RGG domain, are shown enlarged with the RGG repeats indicated by *gray boxes*. *Dots* indicate deleted amino acids. The amino acid sequence of the RGG domain and mutant derivatives is displayed in supplemental Fig. 1. The *drawing* is not to scale. *Right column* (% FAT cells) indicates the % of cells that acquired the FAT phenotype (see text for details) 16 h after transfection with dsRNA homologous to the 5′ UTR of α-tubulin mRNA. Each mutant cell line was challenged with non-saturating amounts of dsRNA (0.5 or 1.0 μg of dsRNA per transfection), and the percentage of FAT cells was normalized to the response of cells expressing wt *Tb*AGO1, which was set at 100%. The value of <5% FAT cells indicates that the RNAi response was severely inhibited; this is the minimal value at or above which the FAT cell phenotype is informative.

(16). Morpholino oligonucleotides (500 μM final concentration) were delivered to trypanosomes by electroporation (35).

RESULTS

The Size of the TbAGO1 RGG Domain and the Presence of Arginine Residues Are Important Determinants for RNAi Competency—One of the striking features of the *T. brucei* AGO1 N-terminal domain is the high representation of arginine-glycine-glycine (RGG) motifs, which make up almost 50% of the first 59 amino acids (16, 36). In particular, between positions 9 and 59 there are 10 RGG motifs, which are part of an 11-amino acid repeating unit with the consensus sequence G(Y/R)RGGRGGG(E/F)G (Fig. 1 and supplemental Fig. 1). Our previous experiments with a mutant AGO1 protein missing amino acids 2–68 (ΔRGG mutant) resulted in a severe impairment of the RNAi response and nearly abolished the association of *Tb*AGO1 with polyribosomes (13). To gain further insight into the functional determinants contained within the *Tb*AGO1 amino terminus, we first tested whether the number of RGG motifs is important for AGO1 function. To this end we generated a series of deletions by removing 11 amino acids at a time starting at position 59 and progressing toward the very N terminus (Fig. 1 and supplemental Fig. 1). Deletion mutants were constructed in an AGO1 complementation vector that was designed to integrate by homologous recombination at the endogenous *TbAGO1* locus of *ago1*$^{-/-}$ cells, using sequences flanking the *AGO1* ORF as recombination targets (13). As a positive control we used the parental *AGO1* gene (*wt*, Fig. 1) assembled in the same complementation vector and similarly integrated in the genome. Semi-quantitative Western blot analysis showed no major differences in the expression levels of wild-type and mutant AGO1 proteins (see Fig. 4*A*). Next, we transfected α-tubulin dsRNA into the various cell lines and determined the number of FAT cells (cells blocked in cytokinesis) that resulted from the down-regulation of α-tubulin synthesis (37). In our standard assay FAT cells, which are non-dividing and easily recognized due the presence of multiple nuclei, flagella, and mitochondrial genomes (kinetoplasts), are counted at the optical microscope 16 h post-transfection. We have previously shown that the magnitude of the FAT phenotype correlates well with the extent of α-tubulin mRNA degradation (17). For instance, in wild-type cells 70–80% degradation of α-tubulin mRNA is manifested by ~50–70% FAT cells. Thus, the measurement of FAT cells serves as a reporter phenotype for RNAi efficiency. The results shown in the *right column* of Fig. 1 were obtained by transfecting non-saturating amounts of α-tubulin dsRNA, and for each mutant the value was normalized relative to the performance of the cell line complemented with wild-type *TbAGO1*, which was set at 100%. By this analysis we observed that progressive deletion of the RGG domain affected RNAi efficiency in a gradual fashion. Specifically, deletion of amino acids 49–59 or 38–59 resulted in a decrease of RNAi efficiency to ~60% of wild-type levels. A further reduction to 35 and 23% was observed for mutants Δ27–59 and Δ16–59, respectively. Finally, dsRNA challenge of cells expressing *Tb*AGO1 mutants devoid of the RGG motifs (Δ7–59), as well as flanking residues (Δ2–59 and Δ7–68), led to <5% FAT cells, which we set as the minimal value at which the FAT phenotype can be reliably assigned. It is important to note that by this assay the performance of the Δ7–59, Δ2–59, and Δ7–68 mutants was indistinguishable from that of the ΔRGG mutant, which was analyzed in our previous study (13).

It is well established that RGG domains can function as modules for protein-protein interactions, and, in the case of human FMRP, the RGG domain has the ability to bind G-quartet-containing RNAs (38, 39). Thus, RGG domains appear to be bifunctional modules that can interact with both proteins and RNAs. Additionally, arginine residues in RGG motifs have the potential to be post-translationally modified by protein arginine *N*-methyltransferases (40, 41). These enzymes add one or two methyl groups to the terminal guanidine nitrogen atoms of arginine thus generating monomethylarginine, asymmetric dimethylarginine, or symmetric dimethylarginine. Because arginine methylation can act as a positive or negative regulator of protein-protein interactions, it was relevant to determine whether arginines in the N-terminal domain of *Tb*AGO1 carry any methyl groups. We initially took advantage of the well established Y12 monoclonal antibody, which recognizes Sm proteins of spliceosomal small nuclear ribonucleoproteins (42). In particular, Y12 reacts with symmetric dimethylarginine in arginine-glycine dipeptide repeats of Sm proteins (43). As can be seen in Fig. 2*A*, TAP-tagged AGO1 either in a total cytoplasmic extract (*lane 1*) or after affinity purification (*lane 3*) was recognized by monoclonal antibody Y12, suggesting that this antibody reacts with symmetric dimethylarginine-containing epitopes in AGO1. In addition, we tested commercially available antibodies that recognize either symmetric dimethylarginine (SYM11) or asymmetric dimethylarginine (ASYM24). *Tb*AGO1 was recognized by SYM11 (data not shown), support-

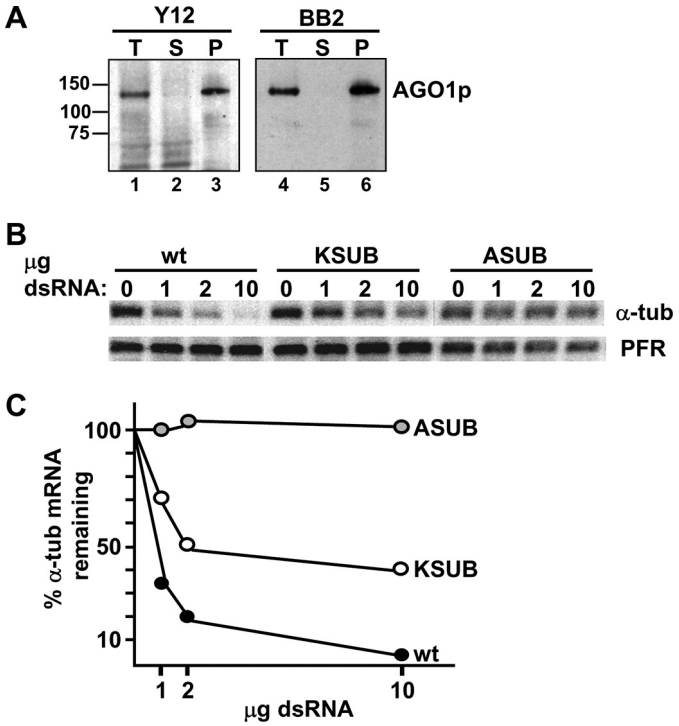

FIGURE 2. *A*, *Tb*AGO1 is recognized by the Y12 monoclonal antibody. Western blot analysis of a total cytoplasmic extract (*T*, *lanes 1* and *4*), supernatant (*S*, *lanes 2* and *5*), and immunoprecipitated AGO1 (*P*, *lanes 3* and *6*) with Y12 or anti-BB2 antibodies. Molecular masses are indicated in kilodaltons. *B*, substitution of arginine residues in the *Tb*AGO1 RGG domain inhibits degradation of α-tubulin mRNA in response to transfection of homologous dsRNA. Wild-type, KSUB, and ASUB cells were electroporated with different amounts (in micrograms) of α-tubulin dsRNA, as indicated *above* each lane or with poly(I-C) (*lane 0*), and total RNA was prepared 2 h after electroporation. The level of α-tubulin mRNA was monitored by Northern blotting with a radiolabeled DNA probe derived from the tubulin coding region. The *bottom panel* shows the hybridization to the paraflagellar rod (*PFR*) protein mRNA that served as a loading control. *C*, quantitation of α-tubulin mRNA degradation. For each cell line α-tubulin mRNA hybridization was quantitated by PhosphorImager analysis and was plotted as the fraction of mRNA remaining 2 h after electroporation, setting as 100% the amount of α-tubulin mRNA present in the samples that received poly(I-C). A representative experiment is shown.

ing the Y12 reactivity. We also observed a low but specific reactivity with ASYM24 (data not shown), suggesting the presence of asymmetrically dimethylated arginine residues.

Potential sites for arginine methylation are glycine-arginine-rich regions, which are often found as repeats. In *Tb*AGO1 such potential sites are clustered at the N terminus in the RGG domain, and this profile is conserved in related trypanosomatid protozoa, namely *T. congolense*, *T. vivax*, and *Leishmania braziliensis* (supplemental Fig. 2). To provide direct evidence for arginine methylation TAP-tagged *Tb*AGO1 was affinity purified, trypsin-digested, and subjected to MALDI-TOF mass spectrometry. Although this led to the preliminary identification of the peptide GG(dmR)GGGEGG(dmR)R, which was assigned to the AGO1 N terminus and predicted to carry two dimethylated arginines, we were not able to determine whether this was asymmetric or symmetric dimethylation. In addition, the highly repetitive nature of the RGG domain was not amenable to an unambiguous identification of modified arginine residues.

Considering the experimental challenges outlined above, we turned to a mutational analysis to evaluate whether the arginine residues in the RGG domain were functionally relevant. We generated two additional mutants (Fig. 1 and supplemental Fig. 1) by substituting all the arginine residues within the first 59 amino acids of *Tb*AGO1 with either lysine (KSUB), a conservative substitution that maintains the positive charge of arginine, or alanine (ASUB), a non-conservative substitution. After the establishment of stable cell lines, we first determined the extent of FAT cell formation (Fig. 1) and found that cells expressing the KSUB mutation produced ~12% FAT cells relative to wild-type cells, whereas cells expressing the ASUB mutant AGO1 protein had a more severe phenotype giving rise to <5% FAT cells. The latter phenotype was similar to mutants missing the entire RGG domain, as well as flanking sequences (Δ2–59, Δ7–68, and ΔRGG). To confirm the phenotype of the KSUB and ASUB mutants, we next determined the extent of degradation of α-tubulin mRNA in response to transfection of different amounts of α-tubulin dsRNA. The Northern blot of Fig. 2*B* and the quantitation of the results in Fig. 2*C* showed that, at the highest dsRNA concentration, mRNA cleavage in KSUB cells was reduced ~5-fold as compared with wild-type cells. Unexpectedly, the ASUB cell line had an undetectable response to α-tubulin dsRNA, a phenotype reminiscent of that of the *ago1*$^{-/-}$ parental cell line, where the RNAi pathway is completely disabled (16).

In conclusion, the above results are consistent with the hypothesis that the size and specifically the arginine residues of the AGO1 N-terminal RGG domain contribute to RNAi efficiency, as gauged by the decreased response to synthetic dsRNA. Our experiments also indicated, likely due to the repetitive nature of the RGG domain, that the first 16 amino acids of this domain, which harbor two RGG motifs, are sufficient for detectable, albeit reduced, AGO1 function. Although the results of our deletion and substitution mutagenesis are consistent with an important functional role of the arginine residues, we found that changing the identity of the arginine residues to lysine led to a much less severe loss of function than arginine to alanine substitutions. It is possible that the severe phenotype of the ASUB mutant may be the result of mis-folding of the N terminus, possibly preventing interaction of *Tb*AGO1 with other cellular component(s), promoting unspecific interactions and/or inhibiting the cleavage activity of *Tb*AGO1.

The Cellular Localization of ASUB and KSUB Mutant Proteins Is Comparable with That of Wild-type AGO1—Our results above suggested that mutating arginine residues in the RGG domain may disrupt arginine methylation. Because arginine methylation of PIWI proteins has been shown to affect its nuclear localization (15), we performed cell fractionation experiments with extracts from wild-type cells and from cells expressing KSUB or ASUB mutant proteins (Fig. 3). The majority of wild-type AGO1 was recovered in the fraction containing cytosolic proteins (*panel A*, *lane 2*), as gauged by the fractionation behavior of cytoplasmic Hsp83 (the homologue of Hsp90). A small proportion of AGO1 was present in the membrane fraction (*lane 4*), where, as predicted, BiP was found exclusively (33). No detectable amount of AGO1 was found in the nuclear fraction (*lane 6*). A comparable fractionation profile was obtained for KSUB and ASUB proteins (*panels B* and *C*,

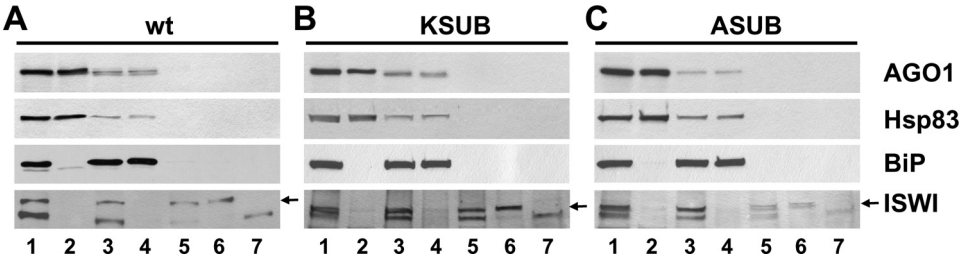

FIGURE 3. **Cell fractionation of cells expressing wild-type AGO1 (*A*), KSUB (*B*), and ASUB (*C*) mutant proteins.** Total cell lysates (*lane 1*) were fractionated into cytosolic proteins (*lane 2*) and a pellet (*lane 3*). Membrane proteins were extracted from the pellet (*lane 4*), and the insoluble material (*lane 5*) was further fractionated into nuclear proteins (*lane 6*) and cytoskeletal proteins (*lane 7*). *Panels* were reacted with an antibody to *Tb*AGO1, Hsp83, BiP, and *Tb*ISWI. *Tb*ISWI is indicated by an *arrow*, just above a cross-reacting band (34).

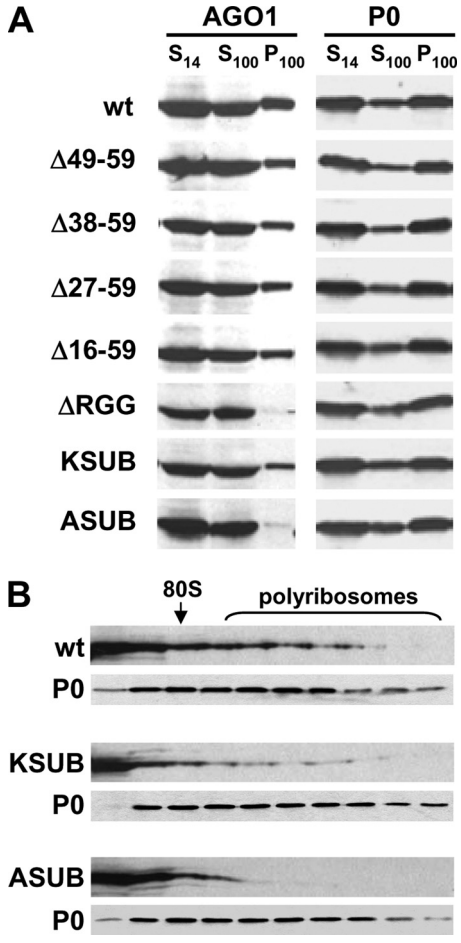

FIGURE 4. *A*, fractionation of wild-type AGO1 and RGG-domain mutant derivatives between soluble and ribosome-enriched material. Extracts were prepared as described (18), and the soluble material after centrifugation at 14,000 × *g* for 10 min (S14) was further fractionated by centrifugation at 100,000 × *g* for 1 h. A 30% sucrose cushion was layered at the bottom of the tubes to minimize contamination of the ribosome-enriched pellet (P100) fraction by the soluble material (S100). Equivalent amounts of S14, S100, and P100 fractions were separated by SDS-PAGE and Western blotted with anti-AGO1 polyclonal antibodies (*AGO1 panels*) or *T. cruzi* anti-P0 polyclonal antibodies (*PO panels*), which monitor the sedimentation of the 60 S ribosomal subunit. *B*, sucrose density gradients of cytoplasmic extracts from cells expressing wild-type (*wt*), KSUB, and ASUB AGO1. The sucrose density gradient fractions were analyzed by Western blots using a rabbit anti-AGO1 polyclonal antibody (*wt*, *KSUB*, and *ASUB panels*) or *T. cruzi* anti-P0 polyclonal antibodies (*PO panels*) to monitor the sedimentation of the 60 S ribosomal subunit.

respectively), indicating that the introduced mutations did not have a major influence on the cellular localization of these proteins.

Determinants for the Association of TbAGO1 with Polyribosomes—We have shown previously that in trypanosomes the majority (~80–90%) of *Tb*AGO1-siRNA complexes are recovered as soluble ribonucleoprotein particles, whereas the remainder ~10–20% of *Tb*AGO1 ribonucleoprotein particles co-sediment with polyribosomes (18). Importantly, the AGO1-polyribosome association was nearly completely abolished in cells expressing the ΔRGG mutant (13). In this context it was of interest to analyze the cellular distribution of the mutant AGO1 proteins we generated in this study. To this end cytoplasmic cell extracts were prepared and centrifuged at 100,000 × *g* for 60 min to separate soluble *Tb*AGO1, which partitions in the S100 supernatant, from polyribosome-associated *Tb*AGO1, which is found in the pellet fraction (P100). Next, equivalent amounts of the input (S14), S100, and P100 fractions were analyzed by Western blotting with a polyclonal anti-*Tb*AGO1 antiserum (Fig. 4*A*, *AGO1 panels*). As a control for loading and ribosome enrichment in the P100 pellet an identical blot was reacted with an antiserum raised against the *T. cruzi* P0 protein, a known component of the large ribosomal subunit (Fig. 4*A*, *P0 panels*). Through this analysis we found that progressive deletion of amino acids 16–59, defined by mutants Δ49–59, Δ38–59, Δ27–59, and Δ16–59, diminished the co-fractionation of *Tb*AGO1 with polyribosomes by ~30–50%, as compared with wild-type AGO1 (*wt panel*). Confirming our previous results, this phenotype was nearly abolished in ΔRGG cells (13). Mutants Δ7–59, Δ2–59, and Δ7–68 behaved similarly to the ΔRGG mutant and were not included in this experiment. In extracts prepared from the KSUB cell line there was a drastic reduction of the amount of *Tb*AGO1 in the P100 pellet, and this was further enhanced in ASUB extracts, which by this assay behaved similarly to the ΔRGG mutant cells. To corroborate the fractionation characteristics of the KSUB and ASUB mutant AGO1 proteins, a cytoplasmic extract was centrifuged through a 15–50% sucrose gradient, and individual fractions were analyzed by Western blotting with a polyclonal anti-AGO1 antibody (Fig. 4*B*). As shown previously (13, 18), wild-type AGO1 partially co-sedimented with polyribosomes. Similar to the fractionation experiments (Fig. 4*A*), there was a substantial reduction in the amount of the KSUB mutant protein co-sedimenting with polyribosomes, and the majority of the ASUB mutant protein was found near the top of the gradient, where soluble material and small ribonucleoprotein particles sediment, and very little, if any of the protein was detected in gradient fractions where polyribosomes sediment (Fig. 4*B*). Thus, although decreasing the overall size of the RGG domain contributed somewhat to the extent of AGO1 co-fractionating with polyribosomes, the effect on this phenotype was most dramatic when the arginine residues within amino acids 2–59 where substituted by lysine or alanine or when the entire RGG domain was deleted (13). The observation that KSUB AGO1, in which the positive charges of the N-terminal domain were

maintained, was greatly reduced in the polyribosome fractions indicated that AGO1 association with polyribosomes is not simply brought about by ionic interactions and thus suggested that this interaction is specific.

As mentioned above, RGG motifs are highly represented at the N terminus of AGO1 proteins from the trypanosomatid protozoa *T. congolense*, *T. vivax*, and *Leishmania braziliensis* (supplemental Fig. 2). Moreover, AGO1 and AGO2 of *Arabidopsis thaliana* have a similar clustering of RGG motifs in the N-terminal domain. Thus, in addition to experimental evidence presented here, sequence conservation can also provide evidence in favor of a functional role for the N-terminal domain of certain Argonautes.

Cell Lines Expressing ΔRGG, KSUB, and ASUB Proteins Accumulate Single-stranded siRNAs Associated with AGO1—The experiments presented above suggested that the N-terminal domain of AGO1 was important either for AGO1 cleavage activity or for promoting an association with polyribosomes. We addressed the first possibility by assaying the capability of mutant proteins to cleave mRNA targets *in vitro*. However, attempts to establish an *in vitro* slicing assay with wild-type *Tb*AGO1 have so far not been successful. Thus, as an alternative approach to gauge the cleavage activity of AGO1, we examined the structure of associated siRNAs. An essential step in RISC activation is the dissociation of the siRNA duplex, which involves removal of the passenger strand and retention of the guide strand. In particular, in systems studied so far, the cleavage activity of Argonaute was required for the generation of single-stranded siRNAs (44–49). Thus, we first monitored the accumulation of endogenous siRNAs derived from Ingi retroposon transcripts in cell lines expressing mutant AGO1 proteins. As noted previously, the abundance of Ingi siRNAs was not visibly affected by the ΔRGG mutation (13), and a similar result was obtained for the KSUB and ASUB mutations (Fig. 5*A*, *lanes 3* and *4*). Next we asked whether the siRNAs formed a ribonucleoprotein complex with the mutated AGO1 proteins. To address this issue, an epitope-tagged version of the ASUB and KSUB protein was immunoprecipitated from a cytoplasmic extract, and the immunoprecipitates were assayed by Northern blotting for the presence of Ingi siRNAs (Fig. 5*B*). This revealed that the majority of Ingi siRNAs were associated with the ASUB and KSUB mutant proteins (*lanes 4* and *6*), comparable to the wild-type protein (*lane 2*) and the previously described ΔRGG mutation (13). To investigate the structure of the siRNAs present in cell lines expressing mutant Argonaute proteins, RNA from an S100 extract was examined using native gel electrophoresis (Fig. 5*C*). The gel mobility of a synthetic ^{32}P-labeled duplex siRNA with and without denaturation prior to electrophoresis served as a marker to identify single- and double-stranded conformations, respectively (*lanes 1* and *2*). In addition, subjecting RNA isolated from a cell line defective in the dissociation of the siRNA duplex to this procedure resulted in the detection of double-stranded siRNAs in the sample not exposed to denaturation.[7] As expected, Ingi siRNAs present in wild-type cells were single stranded (*lane 3*). Similarly, in cell

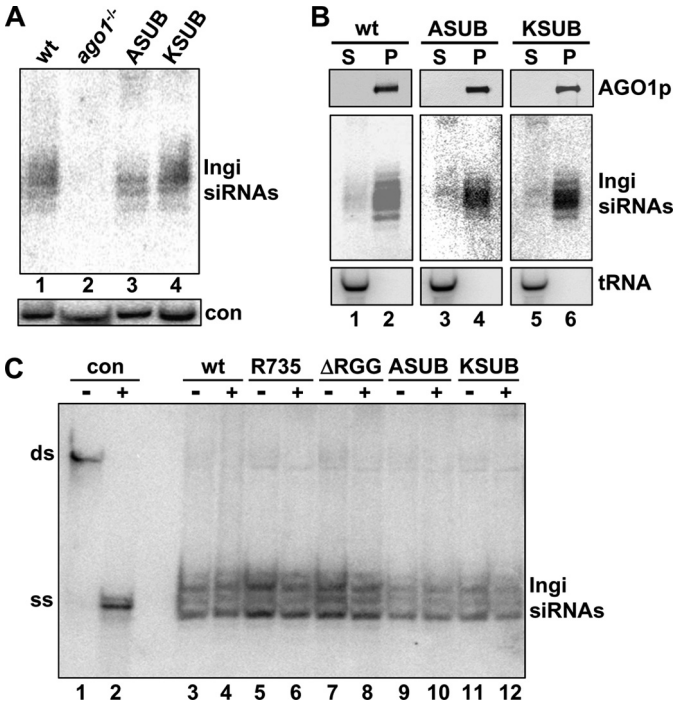

FIGURE 5. **siRNA analysis in cells expressing mutant AGO1 proteins.** *A*, small RNAs isolated from each cell line as indicated was analyzed by Northern blot hybridization with an Ingi radiolabeled probe. Hybridization to tRNA^{Met} served as a loading control (*con*). *B*, association of wild-type (*wt*), ASUB, and KSUB AGO1 with Ingi siRNAs. A cytoplasmic extract from cells expressing N-terminal BB2-tagged AGO1 proteins was subjected to immunoprecipitation with anti-BB2 antibodies, and supernatant (*S*) and pellet (*P*) fractions were processed for Western blot analysis for AGO1 (*upper panel*), Northern blot analysis for Ingi siRNAs (*middle panel*), and tRNA^{Met} (*bottom panel*), which served as a control for immunoprecipitation specificity. *C*, siRNAs in cells expressing wild-type (*wt*), R735, ΔRGG, ASUB, and KSUB AGO1 are single-stranded. RNA from an S100 extract without (−) or with incubation at 95 °C (+) prior to electrophoresis was electrophoresed on a 15% native polyacrylamide gel and hybridized to an oligonucleotide probe complementary to the most abundant Ingi siRNA. A synthetic ^{32}P-labeled siRNA duplex (*con*) served as a marker for migration of single-stranded (*ss*) and double-stranded (*ds*) siRNAs.

lines expressing Arg-735, ΔRGG, KSUB, or ASUB mutant protein, Ingi siRNAs were predominantly single-stranded (*lanes 5*, *7*, *9*, and *11*). Of note is that the Arg-735 mutation, previously shown to be severely defective in the cleavage of target mRNA (13), appeared not to be affected in the generation of single-stranded siRNAs (see "Discussion"). Taken together, our results indicated that siRNA abundance and conversion of duplex siRNA to single-stranded siRNA was not affected by mutations in the N-terminal domain of *Tb*AGO1, suggesting that the mutant proteins most likely retained catalytic activity, although analysis of steady-state siRNAs is not informative about the efficiency of cleavage. Nevertheless, our results provided evidence that the N-terminal RGG domain of AGO1 contains a determinant for the association with polyribosomes.

RNAi-induced Degradation of α-Tubulin mRNA Can Occur When Polyribosomes Are Stabilized and When Ribosome Loading on mRNA Is Inhibited—To investigate whether mRNA cleavage can occur while the mRNA is on polyribosomes, we used cycloheximide, a translation inhibitor that blocks elongation and stabilizes polyribosomes. We chose α-tubulin mRNA as a model, because we (50) and others (51) have previously shown that in cycloheximide-treated trypanosomes the major-

[7] R. L. Barnes, C. Tschudi, and E. Ullu, unpublished observation.

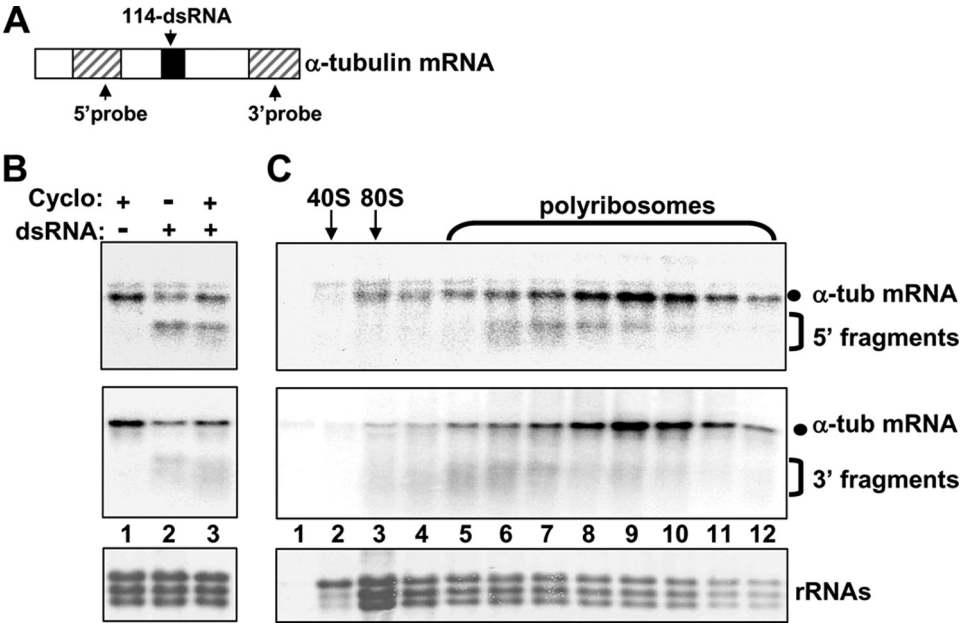

FIGURE 6. **dsRNA-triggered degradation of α-tubulin mRNA can occur in the presence of cycloheximide.** *A*, schematic representation of the coding region of α-tubulin mRNA; the approximate position of the 114-dsRNA is indicated by the *solid box* and the position of the 5′ and 3′ probes used for Northern analysis is indicated by the *stippled boxes*. The *drawing* is not to scale. *B*, Northern blot analysis of α-tubulin mRNA levels with the 5′ or 3′ probe 1 h after transfection with 20 μg of 114-dsRNA (+ *lanes*) or with 20 μg poly(*I-C*) (− *lane*) in the presence or absence of cycloheximide as indicated *above each lane* (see text for details). *C*, sucrose density gradient analysis of the distribution of intact and cleavage fragments of α-tubulin mRNA in cytoplasmic extracts from cells transfected with 114-dsRNA in the presence of cycloheximide. The *bottom panel* shows the methylene blue staining of the large ribosomal RNAs in the sucrose density gradient fractions. The positions of the 40 S subunit and the 80 S monosome are indicated.

ity of α-tubulin mRNA is found on polyribosomes. Trypanosomes were preincubated with cycloheximide for 15 min, washed with electroporation buffer containing cycloheximide, electroporated with α-tubulin dsRNA, and then returned to cell culture media also containing cycloheximide. As a trigger to induce mRNA cleavage we used 114-dsRNA (Fig. 6*A*). This dsRNA is homologous to positions 671–784 of the α-tubulin coding region and thus probes the accessibility to an internal region of the mRNA, which is most likely surrounded and/or bound by ribosomes. In addition, in preliminary experiments we observed that with 114-dsRNA the 5′ and 3′ cleavage products of α-tubulin mRNA were easily detectable (data not shown). Total RNA was prepared 1 h after transfection and analyzed by Northern blotting with probes derived from the 5′ or 3′ ends of α-tubulin mRNA (Fig. 6*B*). The results showed that α-tubulin mRNA cleavage can proceed in the presence of cycloheximide, albeit at a reduced level, *i.e.* an ~30% reduction in mRNA degradation (Fig. 6*B*). At the same time, we prepared a cytoplasmic extract from the cells transfected with 114-dsRNA in the presence of cycloheximide and monitored the sedimentation behavior of intact α-tubulin mRNA and of the cleavage products by sucrose density gradient centrifugation (Fig. 6*C*). Northern blot analysis of individual fractions showed that ~95% of intact α-tubulin mRNA co-sedimented with polyribosomes (fractions 5–12). Interestingly, we also observed that the mRNA cleavage products sedimented as large ribonucleoprotein complexes with the 5′ and 3′ fragments revealing distinct fractionation behaviors. Whether these fragments were still associated with ribosomes or were part of mRNA degradation complexes was not investigated further. Nevertheless, this experiment showed that the target α-tubulin mRNA was mostly associated with ribosomes at the time of cleavage, indicating that RNAi can target mRNA in this environment.

The above results raised the question whether the association of mRNA with polyribosomes was a prerequisite for the RNAi response. To address this issue, we used pactamycin, which allows elongating ribosomes to finish translation and dissociate from the mRNA, but translation initiation is inhibited and, consequently, polyribosomes are depleted. Indeed, our previous studies showed that pactamycin treatment of trypanosomes resulted in the accumulation of non-translating 80 S ribosomes and the disappearance of large polyribosomes (18). Consistent with ribosome run-off, upon treatment with pactamycin α-tubulin mRNA shifted from the heavier to the lighter fractions of a sucrose density gradient (data not shown). Thus, cells were preincubated with pactamycin for 15 min, washed with pactamycin-containing buffer, and electroporated with dsRNA homologous to the 5′ UTR of α-tubulin mRNA, which monitors the accessibility of the mRNA in the region preceding the translation initiation codon (Fig. 7*A*) and incubated in pactamycin-containing medium for 1 or 2 h. The Northern blots in Fig. 7*B* showed that mRNA cleavage can occur in the presence of pactamycin, although there was a reduction of ~1.5-fold in cleavage efficiency as compared with untreated control cells. Of note, in pactamycin-treated cells there was accumulation of a smaller α-tubulin RNA species (indicated by an *asterisk*), which represents the 3′ cleavage product, because it does not hybridize to a 5′ UTR probe (data not shown). The stabilization of this fragment was pactamycin-specific, as it was not observed with cycloheximide or puromycin treatment (data not shown).

Our result that RNAi can proceed in the absence of ongoing translation is in agreement with previous reports in mammalian cells (20, 21). However, we consistently found that inhibition of bulk protein synthesis by cycloheximide or pactamycin resulted in reduction of the RNAi response to transfected dsRNA. We think this effect is most likely due to inhibition of AGO1 synthesis, because we have previously shown that blocking synthesis of AGO1 by various means reduces the RNAi response to transfected dsRNA (35). In conclusion, our experiments suggest that RNAi-mediated mRNA cleavage in trypanosomes can occur on mRNA associated with ribosomes, as well as when most ribosomes are disengaged from the mRNA. The latter observation was consistent with our result

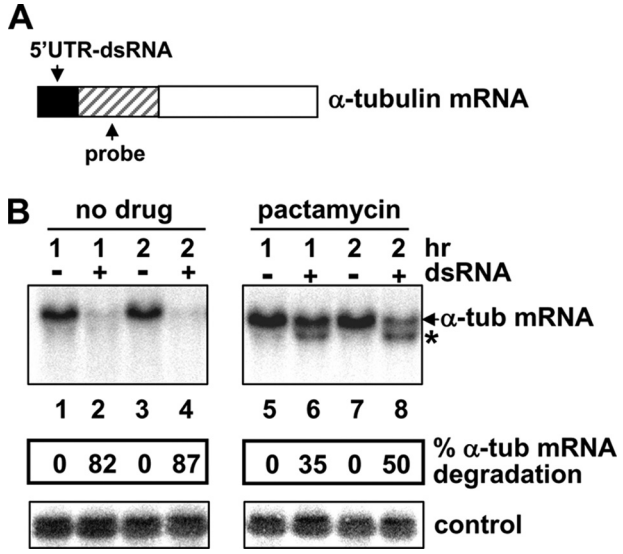

FIGURE 7. *A*, schematic representation of α-tubulin mRNA showing the position of the 5′ UTR dsRNA trigger (*solid box*) and the sequences corresponding to the 5′ tubulin probe (*stippled box*). *B*, RNAi of α-tubulin mRNA can proceed in the presence of pactamycin. Northern blot hybridization of RNA isolated from cells electroporated with dsRNA homologous to the α-tubulin 5′ UTR. Cells were preincubated with no drug (*no drug*) or with 200 μg/ml pactamycin (*pactamycin*) for 15 min and then 10 μg of poly(IC) (− *lanes*) or 10 μg of 5′ UTR dsRNA (+ *lanes*) was electroporated. Incubation was continued in medium with or without the drug for 1 or 2 h, as indicated *above each lane*. 10 μg of total RNA was electrophoresed through a 1.5% agarose-formaldehyde gel and then analyzed by Northern blot hybridization with a tubulin probe, corresponding to nucleotides 1–300 of the α-tubulin coding region. A smaller α-tubulin RNA species, indicated by an *asterisk*, represents the 3′ cleavage product. Each membrane shown in *B* was stripped and rehybridized with a probe detecting the procyclin mRNA as a loading control (control). A similar result was obtained using the 114-dsRNA trigger.

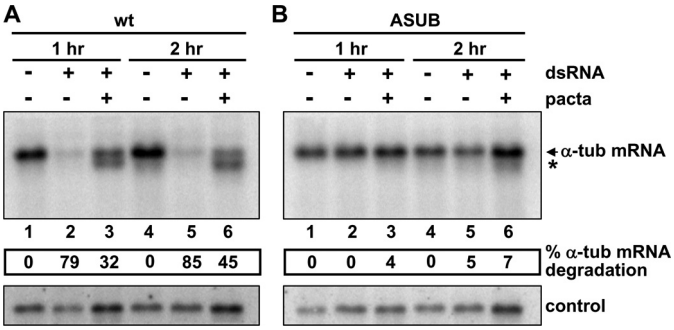

FIGURE 8. **RNAi of α-tubulin mRNA in the presence of pactamycin.** *A*, Northern blot hybridization of RNA isolated from wild-type cells electroporated with dsRNA homologous to the α-tubulin 5′ UTR essentially as described in Fig. 7. *B*, Northern blot hybridization of RNA isolated from cells expressing ASUB AGO1 and exposed to dsRNA and pactamycin (*pacta*) as indicated. A smaller α-tubulin RNA species, indicated by an *asterisk*, represents the 3′ cleavage product. Each membrane shown was stripped and rehybridized with a probe detecting the procyclin mRNA as a loading control (control).

that the RGG mutant retained some cleavage activity, although their polyribosome association is drastically reduced.

Sequestering mRNAs from the Translational Machinery Does Not Allow the ASUB Mutant to Target Tubulin mRNA—The above experiments with pactamycin provided us with an experimental system to test whether the ASUB mutant was able to cleave α-tubulin mRNA under conditions when most ribosomes are disengaged from mRNAs. Thus, we repeated the pactamycin experiments described in Fig. 7 with cells expressing the ASUB mutant protein (Fig. 8). The Northern blot of RNA isolated from wild-type cells mirrored our above results in that mRNA cleavage occurred in the presence of pactamycin, although there was some reduction in cleavage efficiency. On the other hand, pactamycin treatment of ASUB cells had little or no effect on the degradation of α-tubulin mRNA, *i.e.* there was no significant cleavage of target mRNA in the presence or absence of pactamycin (Fig. 8*B*).

The RNAi Response Is Partially Inhibited when Tubulin mRNAs Are Sequestered from Translation—To further analyze the accessibility of mRNA to the RNAi machinery, we investigated the effect of sequestering α- or β-tubulin mRNA from translation by employing antisense morpholino oligonucleotides, which when annealed at or nearby the AUG initiation codon specifically block mRNA translation. Morpholino oligonucleotides, complementary to positions −20 to +5 of α-tubulin mRNA relative to the AUG initiation codon (αtub1 oligonucleotide) and to positions −20 to +5 of β-tubulin mRNA relative to the AUG initiation codon (βtub1 oligonucleotide) or a control morpholino oligonucleotide with an unrelated sequence, were individually electroporated into cells. We first tested whether the antisense morpholino oligonucleotides were efficient blockers of α- and β-tubulin protein synthesis. To this end at 1 or 2 h post-transfection cells were pulse-labeled for 15 min with [^{35}S]methionine, and the radiolabeled proteins were separated by SDS-PAGE (Fig. 9*A*). As a control, cells were transfected with α-tubulin 114-dsRNA (*lane 8*) or β-tubulin BT4-dsRNA (homologous to the last 400 nucleotides of the β-tubulin coding region; *lane 5*). We found that already at 1 h post-transfection the synthesis of α- or β-tubulin protein was drastically reduced by treatment with the corresponding morpholino antisense oligonucleotides and remained low after 2 h of growth (Fig. 9*A*). Next, cells were transfected with the morpholino antisense oligonucleotide plus the corresponding dsRNA and the extent of α- or β-tubulin mRNA degradation was evaluated by Northern blot hybridization (Fig. 9, *B* and *C*) at 1 or 2 h after transfection. The results showed that, as compared with the control oligonucleotide, the specific morpholino antisense oligonucleotides had a negative impact on the extent of α- or β-tubulin mRNA degradation, with 30% to 50% inhibition in three different experiments. Although other interpretations are possible, perhaps the morpholino oligonucleotide-bound mRNAs are less accessible to the RNAi machinery, because they are in a compartment and/or in a ribonucleoprotein complex that partially shields them from the attack of RISC. Similarly, it was shown that in *Drosophila* oocytes the endogenous maternal mRNAs, which are segregated from translation, are not sensitive to RNAi-induced degradation (26). In conclusion, the morpholino antisense oligonucleotides efficiently segregated tubulin mRNAs from translation, as shown by the inhibition of α- and β-tubulin synthesis, and under these conditions α- and β-tubulin mRNAs were less sensitive to dsRNA-mediated cleavage. Our results indicated that translation *per se* is not a requirement for RNAi. Thus, RNAi can proceed on mRNA on polysomes, as well as on mRNA that is not associated with ribosomes.

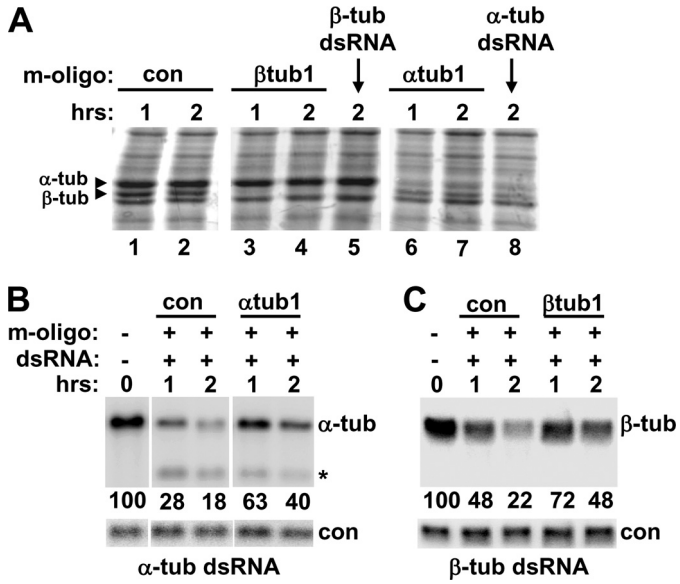

FIGURE 9. *A*, morpholino antisense oligonucleotides sequester α- or β-tubulin mRNA from translation. 10^8 trypanosomes were electroporated with 10 nmol of morpholino oligonucleotide αtub1 (complementary to positions −20 to +5 of α-tubulin mRNA with respect to the AUG initiation codon), βtub1 (complementary to positions −20 to +5 of β-tubulin mRNA with respect to the AUG initiation codon), or control (an oligonucleotide of unrelated sequence) or with α- or β-tubulin dsRNA (114-dsRNA for α-tubulin and BT2-dsRNA for β-tubulin, corresponding to positions 350–690 of the β-tubulin coding region). 1 or 2 h after transfection the cells were pulse-labeled for 15 min with [^{35}S]methionine, and following lysis with SDS-loading buffer the radiolabeled proteins were separated by PAGE as described (54). The position of α- and β-tubulin is indicated and supported by the disappearance of the corresponding band upon transfection with homologous dsRNA (*lanes 5* and *8*). The autoradiogram of the dried gel is shown. *B* and *C*, co-transfection of morpholino antisense oligonucleotides with homologous dsRNA dampens the RNAi response. The identity of the morpholino oligonucleotides and the dsRNA is indicated *above each lane* and at the *bottom of each panel*, respectively. RNA was extracted 1 or 2 h after transfection and analyzed by Northern blot hybridization with the α-tubulin 5′ tubulin probe (see Fig. 6) and a β-tubulin probe corresponding to positions 1050–1340 of β-tubulin mRNA. Each of the membranes shown in *B* and *C* was stripped and rehybridized with a procyclin probe as a loading control (*con*).

DISCUSSION

The findings presented in this work argue that the N-terminal RGG domain significantly contributes to the function of *Tb*AGO1 *in vivo*. Deletions and substitution in the RGG domain reduced the efficiency of the RNAi response to transfected dsRNA, as well as the functioning of the endogenous RNAi pathway, as shown by the inability of some of the mutants to correct the up-regulation of Ingi retroposon transcripts in *ago1*$^{-/-}$ cells (supplemental Fig. 3). The specific role of the RGG domain in *Tb*AGO1 function is at present only a matter of speculation and will require further investigation. Nevertheless, the RGG domain and specifically the arginine residues constitute a determinant for the association of *Tb*AGO1 with polyribosomes. It is possible that other sequences in *Tb*AGO1 are involved in this phenomenon, because appending the RGG domain to GFP did not result in polyribosome targeting of the fusion protein.[6] One consideration is that some of the arginine residues might need to be methylated and that sequences downstream from the RGG domain are necessary for substrate recognition by protein arginine methyltransferases (PRMTs). Although certain PRMTs have been characterized in trypanosomes (52, 53), down-regulation of these enzymes affects many proteins in the cell making it difficult to draw specific connections to the RNAi pathway. Nevertheless, during the preparation of this report, arginine methylation was reported for PIWI proteins in the mouse and fly (14, 15), and in the fly these modifications are carried out by PRMT5 (14).

Our past and present experiments strongly support the hypothesis that the association of *Tb*AGO1 with polyribosomes is functionally relevant in the RNAi pathway: it depends on specific sequences, and it appears that, although mutations in the RGG domain drastically affected polyribosome association, they did not interfere with the resolution of duplex siRNAs to single-stranded siRNAs. Because this step in RISC formation has been shown to require the catalytic activity of Argonaute (37–42), one possible explanation is that the mutant AGO1 proteins retained some activity to convert siRNAs and to cleave target mRNA. However, we cannot exclude the possibility that Argonaute in *T. brucei* depends on an auxiliary protein for the dissociation of siRNA duplexes.

Our current evidence is most consistent with the hypothesis that in steady-state conditions *Tb*AGO1 interacts with some, yet to be identified component of translating ribosomes. Similar to *Drosophila* AGO2-slicer (7), the *Tb*AGO1 ribonucleoprotein can be released from polyribosome-enriched pellets by extraction with 400 mM salt (18), suggestive of a protein-protein or protein-RNA interaction, but not supporting an RNA-RNA interface. The association of *Tb*AGO1 with polyribosomes does not appear to depend on the target mRNA being present in polyribosomes, as we have shown that both sense and antisense MT40 siRNAs co-sediment with polyribosomes (18). In addition, GFP-derived siRNAs are found on polyribosomes even when the target mRNA is not expressed. However, we cannot exclude the possibility that at any time a small proportion of *Tb*AGO1 interacts with the target mRNA via hydrogen bonding with the guide siRNA, along the line that miRNAs in human cells have been shown to associate with polyribosomes in an mRNA-dependent manner (29). Our observation that α-tubulin mRNA can be cleaved in the polyribosome milieu supports this scenario. It is possible that target binding and cleavage by *Tb*AGO1 occur very rapidly once contact is made, thus making it difficult to observe an AGO-mRNA interaction in steady-state conditions. Why does *Tb*AGO1 interact with polyribosomes even though mRNA does not have to be associated with ribosomes to be a substrate for RNAi? We have previously shown that retroposon-derived siRNAs, the hallmark of the endogenous RNAi pathway, co-sediment with polyribosome-enriched material and are the major constituents of siRNAs sequenced from polyribosomes (31). We propose that *Tb*AGO1 on polyribosomes functions as a sentinel ready for action should potentially dangerous retroposon transcripts become associated with polyribosomes.

Acknowledgments—We thank Drs. Gloria Rudenko and Jay Bangs for antibodies.

REFERENCES

1. Farazi, T. A., Juranek, S. A., and Tuschl, T. (2008) *Development* **135,** 1201–1214

2. Cerutti, H., and Casas-Mollano, J. A. (2006) *Curr. Genet.* **50,** 81–99
3. Tolia, N. H., and Joshua-Tor, L. (2007) *Nat. Chem. Biol.* **3,** 36–43
4. Hutvagner, G., and Simard, M. J. (2008) *Nat. Rev. Mol. Cell Biol.* **9,** 22–32
5. Hammond, S. M., Boettcher, S., Caudy, A. A., Kobayashi, R., and Hannon, G. J. (2001) *Science* **293,** 1146–1150
6. Meister, G., Landthaler, M., Patkaniowska, A., Dorsett, Y., Teng, G., and Tuschl, T. (2004) *Mol. Cell* **15,** 185–197
7. Hammond, S. M., Bernstein, E., Beach, D., and Hannon, G. J. (2000) *Nature* **404,** 293–296
8. Kiriakidou, M., Tan, G. S., Lamprinaki, S., De Planell-Saguer, M., Nelson, P. T., and Mourelatos, Z. (2007) *Cell* **129,** 1141–1151
9. Eulalio, A., Huntzinger, E., and Izaurralde, E. (2008) *Nat. Struct. Mol. Biol.* **15,** 346–353
10. Kinch, L. N., and Grishin, N. V. (2009) *Biol. Direct.* **4,** 2
11. Meyer, W. J., Schreiber, S., Guo, Y., Volkmann, T., Welte, M. A., and Müller,H. A. (2006) *PLoS Genet.* **2,** e134
12. Stoica, C., Carmichael, J. B., Parker, H., Pare, J., and Hobman, T. C. (2006) *J. Biol. Chem.* **281,** 37646–37651
13. Shi, H., Ullu, E., and Tschudi, C. (2004) *J. Biol. Chem.* **279,** 49889–49893
14. Kirino, Y., Kim, N., de Planell-Saguer, M., Khandros, E., Chiorean, S., Klein, P. S., Rigoutsos, I., Jongens, T. A., and Mourelatos, Z. (2009) *Nat. Cell Biol.* **11,** 652–658
15. Vagin, V. V., Wohlschlegel, J., Qu, J., Jonsson, Z., Huang, X., Chuma, S., Girard, A., Sachidanandam, R., Hannon, G. J., and Aravin, A. A. (2009) *Genes Dev.* **23,** 1749–1762
16. Shi, H., Djikeng, A., Tschudi, C., and Ullu, E. (2004) *Mol. Cell Biol.* **24,** 420–427
17. Shi, H., Tschudi, C., and Ullu, E. (2006) *RNA* **12,** 943–947
18. Djikeng, A., Shi, H., Tschudi, C., Shen, S., and Ullu, E. (2003) *RNA* **9,** 802–808
19. Tuschl, T., Zamore, P. D., Lehmann, R., Bartel, D. P., and Sharp, P. A. (1999) *Genes Dev.* **13,** 3191–3197
20. Gu, S., and Rossi, J. J. (2005) *RNA* **11,** 38–44
21. Sen, G. L., Wehrman, T. S., and Blau, H. M. (2005) *Differentiation* **73,** 287–293
22. Caudy, A. A., Myers, M., Hannon, G. J., and Hammond, S. M. (2002) *Genes Dev.* **16,** 2491–2496
23. Caudy, A. A., Ketting, R. F., Hammond, S. M., Denli, A. M., Bathoorn, A. M., Tops, B. B., Silva, J. M., Myers, M. M., Hannon, G. J., and Plasterk, R. H. (2003) *Nature* **425,** 411–414
24. Pham, J. W., Pellino, J. L., Lee, Y. S., Carthew, R. W., and Sontheimer, E. J. (2004) *Cell* **117,** 83–94
25. Ishizuka, A., Siomi, M. C., and Siomi, H. (2002) *Genes Dev.* **16,** 2497–2508
26. Kennerdell, J. R., Yamaguchi, S., and Carthew, R. W. (2002) *Genes Dev.* **16,** 1884–1889
27. Nilsen, T. W. (2007) *Trends Genet.* **23,** 243–249
28. Vasudevan, S., Tong, Y., and Steitz, J. A. (2007) *Science* **318,** 1931–1934
29. Maroney, P. A., Yu, Y., Fisher, J., and Nilsen, T. W. (2006) *Nat. Struct. Mol. Biol.* **13,** 1102–1107
30. Nottrott, S., Simard, M. J., and Richter, J. D. (2006) *Nat. Struct. Mol. Biol.* **13,** 1108–1114
31. Djikeng, A., Shi, H., Tschudi, C., and Ullu, E. (2001) *RNA* **7,** 1522–1530
32. Puig, O., Caspary, F., Rigaut, G., Rutz, B., Bouveret, E., Bragado-Nilsson, E., Wilm, M., and Séraphin, B. (2001) *Methods* **24,** 218–229
33. Bangs, J. D., Uyetake, L., Brickman, M. J., Balber, A. E., and Boothroyd, J. C. (1993) *J. Cell Sci.* **105,** 1101–1113
34. Hughes, K., Wand, M., Foulston, L., Young, R., Harley, K., Terry, S., Ersfeld, K., and Rudenko, G. (2007) *EMBO J.* **26,** 2400–2410
35. Shi, H., Tschudi, C., and Ullu, E. (2007) *RNA* **13,** 1132–1139
36. Durand-Dubief, M., and Bastin, P. (2003) *BMC Biol.* **1,** 2
37. Ngô, H., Tschudi, C., Gull, K., and Ullu, E. (1998) *Proc. Natl. Acad. Sci. U.S.A.* **95,** 14687–14692
38. Darnell, J. C., Jensen, K. B., Jin, P., Brown, V., Warren, S. T., and Darnell, R. B. (2001) *Cell* **107,** 489–499
39. Ramos, A., Hollingworth, D., and Pastore, A. (2003) *RNA* **9,** 1198–1207
40. Bedford, M. T. (2007) *J. Cell Sci.* **120,** 4243–4246
41. Bedford, M. T., and Clarke, S. G. (2009) *Mol. Cell* **33,** 1–13
42. Lerner, M. R., and Steitz, J. A. (1979) *Proc. Natl. Acad. Sci. U.S.A.* **76,** 5495–5499
43. Brahms, H., Raymackers, J., Union, A., de Keyser, F., Meheus, L., and Lührmann, R. (2000) *J. Biol. Chem.* **275,** 17122–17129
44. Miyoshi, K., Tsukumo, H., Nagami, T., Siomi, H., and Siomi, M. C. (2005) *Genes Dev.* **19,** 2837–2848
45. Maiti, M., Lee, H. C., and Liu, Y. (2007) *Genes Dev.* **21,** 590–600
46. Leuschner, P. J., Ameres, S. L., Kueng, S., and Martinez, J. (2006) *EMBO Rep.* **7,** 314–320
47. Matranga, C., Tomari, Y., Shin, C., Bartel, D. P., and Zamore, P. D. (2005) *Cell* **123,** 607–620
48. Rand, T. A., Petersen, S., Du, F., and Wang, X. (2005) *Cell* **123,** 621–629
49. Kim, K., Lee, Y. S., and Carthew, R. W. (2007) *RNA* **13,** 22–29
50. Ullu, E., Djikeng, A., Shi, H., and Tschudi, C. (2002) *Philos. Trans. R Soc. Lond. B Biol. Sci.* **357,** 65–70
51. Brecht, M., and Parsons, M. (1998) *Mol. Biochem. Parasitol.* **97,** 189–198
52. Pelletier, M., Pasternack, D. A., and Read, L. K. (2005) *Mol. Biochem. Parasitol.* **144,** 206–217
53. Pasternack, D. A., Sayegh, J., Clarke, S., and Read, L. K. (2007) *Eukaryot. Cell* **6,** 1665–1681
54. Stieger, J., Wyler, T., and Seebeck, T. (1984) *J. Biol. Chem.* **259,** 4596–4602